AGU PUBLICATIONS

JGR

Journal of Geophysical Research: Oceans

RESEARCH ARTICLE

10.1002/2015JC011228

Key Points:
- Freshening and lightening in the Bransfield Strait deep waters is observed
- Interannual thermohaline variability is caused by changes in the inflow of source water masses
- Salinity and neutral density were negatively correlated with the Southern Annular Mode

Supporting Information:
- Supporting Information S1
- Figure S1

Correspondence to:
T. S. Dotto,
tiago.dotto@noc.soton.ac.uk

Citation:
Dotto, T. S., R. Kerr, M. M. Mata, and C. A. E. Garcia (2016), Multidecadal freshening and lightening in the deep waters of the Bransfield Strait, Antarctica, *J. Geophys. Res. Oceans*, *121*, 3741–3756, doi:10.1002/2015JC011228.

Received 12 AUG 2015
Accepted 5 MAY 2016
Accepted article online 9 MAY 2016
Published online 2 JUN 2016

Multidecadal freshening and lightening in the deep waters of the Bransfield Strait, Antarctica

Tiago S. Dotto[1,2], Rodrigo Kerr[1], Mauricio M. Mata[1], and Carlos A. E. Garcia[1]

[1]Laboratório de Estudos dos Oceanos e Clima, Instituto de Oceanografia, Universidade Federal do Rio Grande, Rio Grande, Brazil, [2]Now at Ocean and Earth Science, National Oceanography Centre Southampton, University of Southampton, Southampton, UK

Abstract The deep waters of the Bransfield Strait receive considerable amounts of water from the Weddell Sea continental shelf. The restricted connections to the surrounding ocean and relatively easier access makes the Bransfield Strait an important proxy region for monitoring changes in the dense Weddell Sea shelf water masses, which are an important precursor of Antarctic Bottom Water (AABW). Long-term hydrographic data from the period 1960s–2010s showed freshening and lightening of the deep water masses of the Bransfield Strait, which was likely caused by large freshwater inputs originating from the western shelf of the Weddell Sea. The rates of freshening and lightening were -0.0010 ± 0.0005 yr^{-1} and -0.0016 ± 0.0014 kg m^{-3} yr^{-1} for the central basin, respectively, and -0.0010 ± 0.0006 yr^{-1} and -0.0029 ± 0.0013 kg m^{-3} yr^{-1} for the eastern basin, respectively. The deep waters showed a high degree of interannual thermohaline variability, which appeared to be caused by changes in the proportions of source water mass mixing between the years. Statistically significant negative correlations between salinity/neutral density fields and the Southern Annular Mode (SAM) were observed (-0.56 and -0.62 for the central basin, respectively, and -0.58 and -0.68 for the eastern basin, respectively) between 1980 and 2014. During SAM positive phases, communication between the Weddell Sea and the Bransfield Strait is reduced, which leads to less saline and lighter water masses in the Bransfield Strait; however, the opposite trends are observed during SAM negative phases.

1. Introduction

The Bransfield Strait is located west of the tip of the Antarctic Peninsula (Figure 1a), and this region receives a considerable contribution of cold, dense waters from the continental shelf of the western Weddell Sea [*Wilson et al.*, 1999; *Gordon et al.*, 2000], which is an important region for the formation of Antarctic Bottom Water [*Huhn et al.*, 2008; *Heywood et al.*, 2014; *van Caspel et al.*, 2015]. Relatively shallow topography around the strait (Figure 1a) prevents the mixing of these waters with the surrounding oceans, thus preserving its thermohaline characteristics [*Wilson et al.*, 1999]. After entering the Bransfield Strait, these dense waters sink in one of the three deep basins of the region (western, central or eastern), where they remain with restricted connections to the adjacent seas.

The circulation within the Bransfield Strait is characterized by a cyclonic gyre [e.g., *Zhou et al.*, 2002; *Sangrà et al.*, 2011]. The cold waters from the continental shelf of the Weddell Sea flow into the region around the tip of the Antarctic Peninsula and Joinville Island (Figure 1a) [*von Gyldenfeldt et al.*, 2002; *Thompson et al.*, 2009; *Collares et al.*, 2015], whereas Circumpolar Deep Water (CDW) and warm surface waters from the Bellingshausen Sea enter into the Bransfield Strait mainly at the southwestern passages between (i) the Snow, Smith and Low Islands and the Antarctic Peninsula [*Niiler et al.*, 1991] and between (ii) King George and Elephant Islands (Figure 1a) [*Hofmann et al.*, 1996]. This complex combination of water masses characterizes the thermohaline properties and variability of the deep waters of the Bransfield Strait [e.g., *Clowes*, 1934; *Gordon and Nowlin*, 1978; *Hofmann et al.*, 1996; *Wilson et al.*, 1999; *Gordon et al.*, 2000; *Garcia and Mata*, 2005].

Two varieties of shelf water are the main precursors of the deep water of the Bransfield Strait: High-Salinity Shelf Water (HSSW) and Low-Salinity Shelf Water (LSSW) [e.g., *Gordon and Nowlin*, 1978; *Whitworth et al.*, 1994; *von Gyldenfeldt et al.*, 2002]. Together, these shelf waters account for ~65% and ~90% of the contribution to the eastern and central basin bottom waters, respectively, whereas the final composition

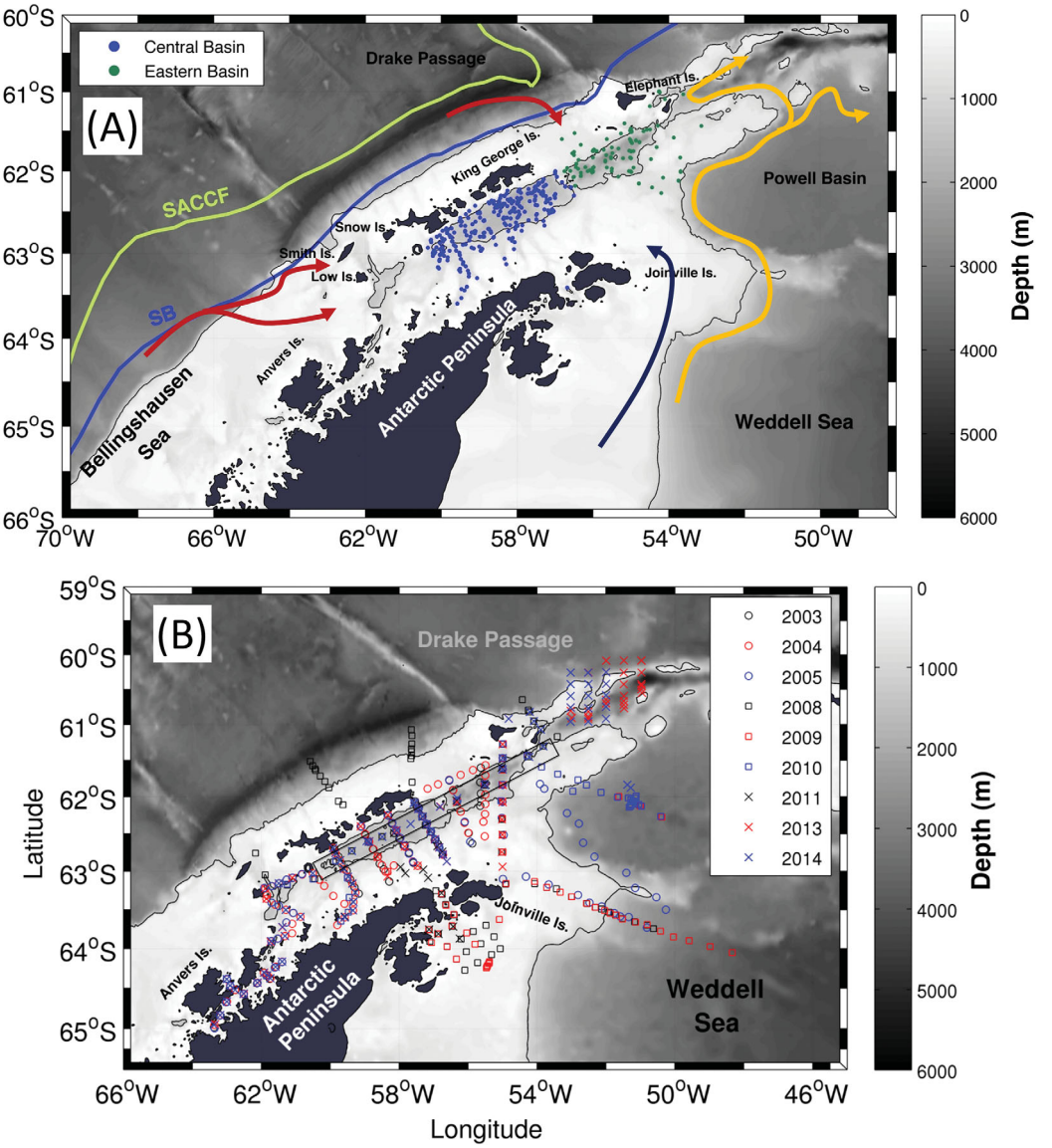

Figure 1. Map and bathymetry of the Bransfield Strait. (a) The colored dots represent all data available for this study. The blue dots and green dots represent the hydrographic stations of the central basin and eastern basin, respectively. The arrows represent the schematic pathways of the Weddell Sea shelf water (dark blue) and Bellingshausen Sea surface water and the Circumpolar Deep Water (red) entering into the strait. The light green and light blue lines represent the mean locations of the Southern Antarctic Circumpolar Current Front (SACCF) and the southern boundary of Antarctic Circumpolar Current (SB), respectively. The orange line is the schematic path of the Antarctic Slope Front and the Weddell Front. The black line is the 1000 m isobath. (b) Map showing the GOAL high-resolution oceanographic data set collected around the tip of Antarctic Peninsula from 2003 to 2014. The black contour rectangle represents the repetition line used in the OMP analysis.

percentage of the Bransfield Strait waters is formed by a mixture of CDW and/or intermediate warm water from the Weddell Sea [*Gordon et al*., 2000]. In particular, the central basin traps the majority of the Weddell Sea shelf waters [*Wilson et al*., 1999; *Gordon et al*., 2000], thereby serving as a proxy region for evaluating thermohaline changes of a key source component of AABW.

Early studies of the Bransfield Strait dating from the beginning of 1900s aimed to characterize the regional hydrographic properties [e.g., *Clowes*, 1934], whereas studies investigating the temporal variability of the deep waters of the region are recent. The Bransfield Strait deep water masses have experienced a general decrease in temperature, salinity, and density from the 1960s to 2000s [*Wilson et al*., 1999; *Garcia and Mata*, 2005; *Azaneu et al*., 2013]. *Garcia and Mata* [2005] showed that between 1980 and 2005, the deep waters (deeper than 1000 m and colder than −1.4°C) of the central basin of the Bransfield Strait had a potential

temperature increase and salinity decrease at rates of $+0.0027$°C yr^{-1} and -0.0014 yr^{-1}, respectively. Conversely, *Azaneu et al*. [2013] considered the Bransfield Strait as a whole and found decreases in potential temperature, salinity, and neutral density of the deep water masses at rates of -0.0278°C yr^{-1}, -0.0012 yr^{-1}, and -0.0013 kg m^{-3} yr^{-1}, respectively, from 1958 to 2010. Both studies concluded that the decrease in salinity was likely caused by the dilution of the shelf waters observed in the western Weddell Sea over the last 50 years because of the intense glacial ice loss in the Antarctic Peninsula [e.g., *Cook et al*., 2005; *Rignot et al*., 2013]. Recent works have shown that freshening trends occurred in the Weddell Sea shelf waters (ranging from -0.0013 yr^{-1} to -0.0053 yr^{-1}) and resulted in a decrease in density from the 1950s–2010s [*Hellmer et al*., 2011; *Azaneu et al*., 2013; *Schmidtko et al*., 2014]. These trends are indicative of changes in the Antarctic hydrological cycles [*Durack et al*., 2012]. The freshening over the continental shelf around Antarctica is likely responsible for the decreased salinity observed in the deep oceans around the deep basins of the world [e.g., *Azaneu et al*., 2013; *Jullion et al*., 2013; *Purkey and Johnson*, 2013; *van Wijk and Rintoul*, 2014].

Changes in the inflow of source water masses into the Bransfield Strait may have caused interannual changes in the thermohaline characteristics of the deep water masses. For example, there is an approximately 5 months lag in the influence of wind stress over the Weddell Gyre on changes in the AABW thermohaline properties within the Drake Passage [*Jullion et al*., 2010]. For the upper ocean, *Renner et al*. [2012] suggested that the connections between the Weddell Sea and areas west of the Antarctic Peninsula are restricted during positive phases of the Southern Annular Mode (SAM) because of stronger westerlies and ocean front shifts near the tip of the Peninsula. Because the strait receives considerable contributions from the Weddell Sea shelf waters, the effects of the SAM on the Weddell Sea atmosphere/ocean circulation may also impact the interannual variability of the deep water masses of the Bransfield Strait.

Here, we used a recent and extensive high-resolution observational data set to examine the spatial and temporal variability in the Bransfield Strait hydrographic properties between 1963 and 2014. The paper is organized as follows: section 2 provides a description of the observational data set and the methods used in this work; section 3 presents the main results with regard to the thermohaline structure of the deep waters of the Bransfield Strait basins, their temporal variability and admixture changes from different sources; section 4 includes a discussion of the study results; and section 5 presents the summary and main conclusions.

2. Data and Methods

2.1. Hydrographic Data Sets

We compiled data from three different sources: (1) the World Ocean Database 2013 (WOD13) [*Boyer et al*., 2013] bottle and conductivity-temperature-depth (CTD) data, (2) the Alfred Wegener Institute CTD data (www.pangaea.de), and (3) the Brazilian High Latitude Oceanography Group (GOAL; www.goal.furg.br) CTD data from 2003 to 2014 (Figure 1b). The WOD13 database includes only measurements considered to be of good quality according to the WOD quality flag criteria [*Johnson et al*., 2013]. Duplicate hydrographic stations appearing in more than one data set and spurious hydrographic data greater than two standard deviations from the mean value of each profile were removed. To avoid the influence of water masses over the continental shelf, only data located in regions where the bathymetry was deeper than 500 m were used. We further divided the data regionally according to the bathymetry and the shallow sills located between the Bransfield Strait basins (Figure 1a). Hereafter, we refer to these regions as the central basin and the eastern basin of the Bransfield Strait (Figure 1a). The western basin was not analyzed because its circulation and thermohaline characteristics are predominantly influenced by water intrusions from the Bellingshausen Sea and its shallow bathymetry does not trap deep waters. For the central (eastern) basin (Figure 1a), years that presented less than three (two) hydrographic stations with $\gamma^n \geq 28.27$ kg m^{-3} were removed from the analysis. The combined data sets covered a period of 52 years (1963–2014) for the central basin and 40 years (1975–2014) for the eastern basin and were restricted to the austral summer (November–March; for the decadal location of the hydrographic stations, please refer to supporting information Figure S1).

The techniques and instrument accuracies related to ocean measurements have changed over the study period. The earliest data were primarily from bottle samples and low-resolution CTD records, whereas the later data were from higher-quality CTDs. The accuracy of the WOD13 CTDs varied from 0.001–0.005°C for temperature and 0.003–0.02 for salinity [*Boyer et al*., 2013]. In general, the GOAL measurements had accuracies of approximately 0.002°C for temperature and 0.003 for salinity [*Azaneu et al*., 2013]. Thus, the accuracy

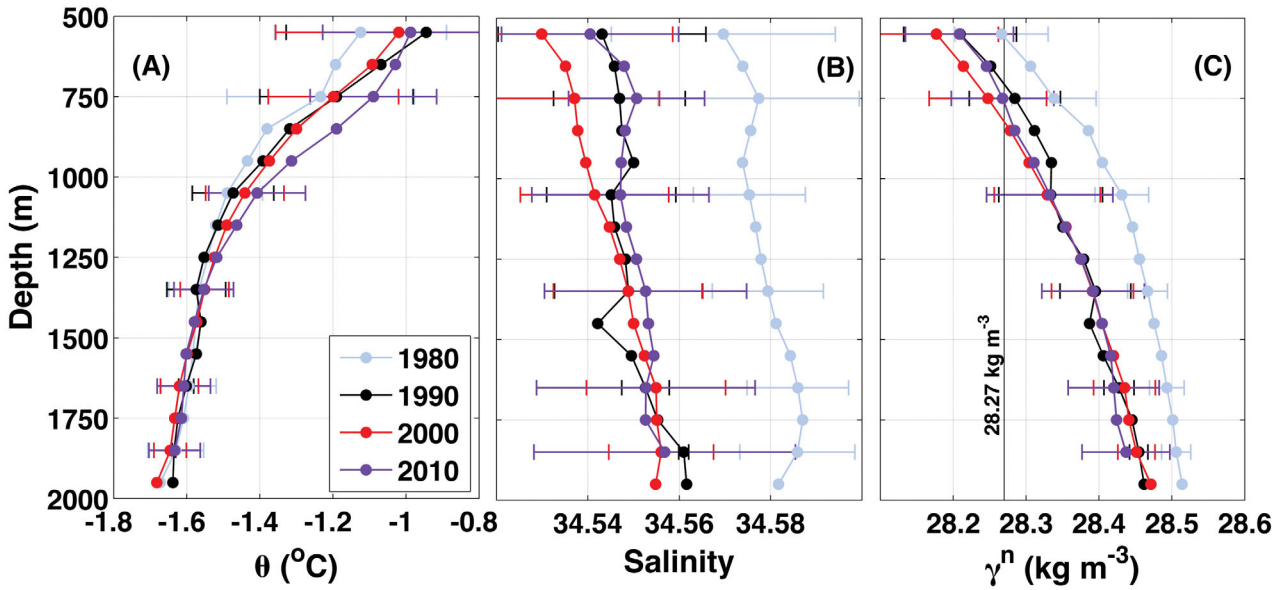

Figure 2. Decadal profiles of the hydrographic parameters for depths greater than 500 m in the central basin. Potential temperature (θ; a), salinity (S; b), and neutral density (γn; c). The decade colors are shown in the legend of Figure 2a. Horizontal bars represent the standard deviations relative to certain chosen depths.

ranges of the CTD data within the combined data set were 0.001–0.005°C for temperature and approximately 0.003–0.02 for salinity.

Four hydrographic parameters were analyzed: potential temperature (θ; °C), salinity (S), neutral density (γ^n; kg m^{-3}), and dissolved oxygen (DO; mL L^{-1}). In this work, the deep waters in the Bransfield Strait were defined as those with $\gamma^n \geq 28.27$ kg m^{-3}, which is characteristic of the dense waters produced around the Antarctic continental margins, including the dense shelf waters [e.g., *Nicholls et al*., 2009] that provide an important source of AABW [e.g., *Orsi et al*., 1999]. The depth of the 28.27 kg m^{-3} isopycnal (calculated from the first depth with $\gamma^n \geq 28.27$ kg m^{-3}) was analyzed and used as a proxy to provide information about the deep water volume shrinkage or expansion.

We analyzed the thermohaline vertical structure of the Bransfield Strait using decadal profiles from the central and eastern basins (Figures 2 and 3). Each decadal profile is the average of individual profiles grouped within their respective decade and binned in 100 m windows from 500 m to the bottom (without the use of the threshold value $\gamma^n \geq 28.27$ kg m^{-3}). We restricted our analysis to the decades between the 1980s and 2010s because earlier decades featured much less usable data.

2.2. Ancillary Data and Quantification of the Deep Water Mass Mixtures

The SAM is the dominant mode of large-scale climate variability in the Southern Ocean [e.g., *Marshall et al*., 2004]. We used observations based the SAM index (http://www.nerc-bas.ac.uk/icd/gjma/sam.html) [*Marshall*, 2003] to study the relationships of the SAM with the thermohaline properties of the Bransfield Strait deep waters.

The Optimum Multiparameter Analysis (OMP) inverse method [*Tomczak and Large*, 1989] was used to quantify the mixing of the water masses from different sources in the deep layers (i.e., depths $>$ 800 m) of the central and eastern basins using GOAL data from 2004–2014 from the repeated hydrographic section. The source water types observed in the mixture of the Bransfield Strait were HSSW, LSSW, and CDW. Because of the paucity of data for the northwestern Weddell Sea continental shelf, the thermohaline index was derived from the literature following *Carmack* [1974], *Carmack and Foster* [1975], *Orsi et al*. [1995], *Weppernig et al*. [1996], and *Robertson et al*. [2002]. The weights used for each parameter were determined according to *Tomczak and Large* [1989]. We followed *Kerr et al*. [2009] and carefully performed sensitivity analyses (not shown) to perturb the defined source water types (Table 1) by adding previously reported trends [e.g., *Robertson et al*., 2002; *Azaneu et al*., 2013] to assess the resulting OMP mixture fractions. The differences among the water mass fractions between the OMP runs were less than 5%. Thus, substantial changes were not observed between the OMP runs by adding long-term changes, thus demonstrating the robustness of

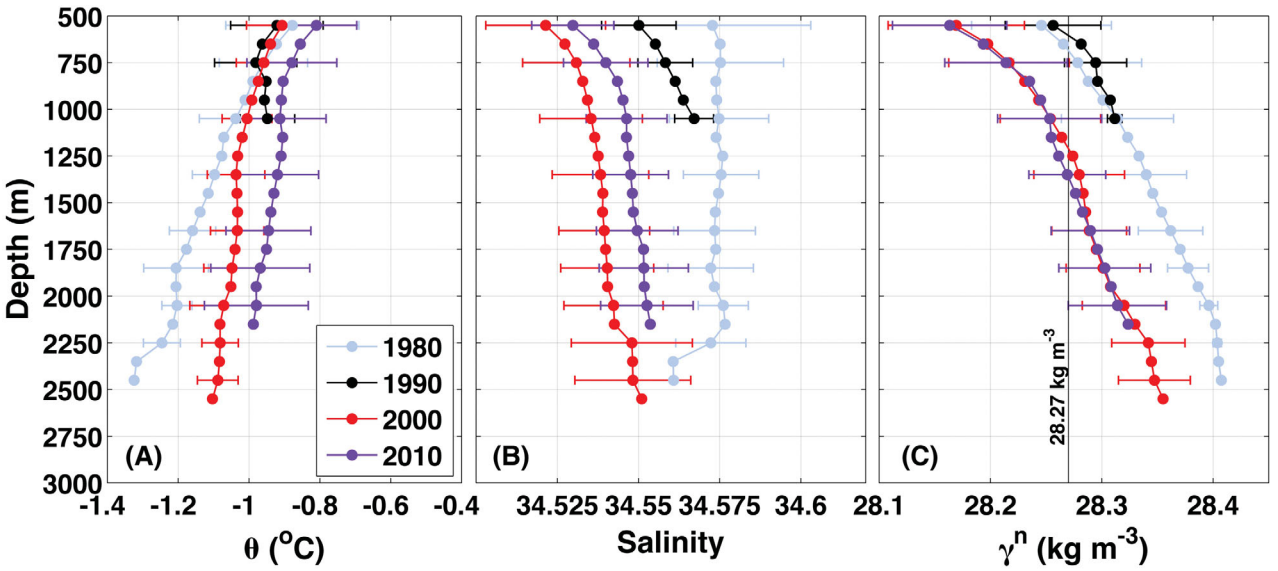

Figure 3. Same as in Figure 2 but for the eastern basin. Note that the scales between the central basin and the eastern basin are different.

the method for inferring temporal water mass variations [e.g., *Leffanue and Tomczak*, 2004; *Tomczak and Liefrink*, 2005; *Kerr et al*., 2009]. The OMP results yielded low mass conservation residual values ($<$ 5%), thus providing additional support for the results.

2.3. Trend Calculations

We followed *Azaneu et al*. [2013] and calculated the annual time series anomalies of seawater properties relative to the decade 2000–2009 for both the central and eastern basins. We chose this decade because it presented the best spatial coverage among the studied decades (supporting information Figure S1). Each vertical property profile was subtracted from the 2000–2009 averaged profile to produce anomaly profiles. Next, we used a second depth threshold of depth $>$ 800 m to select only the deep, dense water masses that may have been less influenced by mixing, thus preserving their "pure" form. The data were grouped into their respective summers, and the average and standard deviations for each year were calculated. The temporal trends determined from linear fits, confidence limits for the estimated trends, and statistical *p* values (at the 95% confidence levels) were determined for each time series.

Sensitivity tests (not shown) were performed to exclude methodology bias. We changed the criteria by relaxing the thresholds for the data per year and "pure" water depths. The most robust results in which the time series signals were conserved and less data were lost, were achieved using the thresholds presented in subsection 2.1 (minimum of three stations per year with $\gamma^n \geq 28.27$ kg m^{-3} in the central basin and two in the eastern basin) and 2.3 (depth higher than 800 m).

3. Results

3.1. Vertical Structure of the Bransfield Strait (1980s–2010s)

A comparison of the vertical profiles between the 1980s and 2010s showed an increase in θ between 500 m and 1000 m (reaching differences of ~0.2°C between 500 m and 800 m; Figure 2a), although between the

Table 1. Source Water-Type Indices, Their Properties (Potential Temperature, θ°C; Salinity, *S*; and Dissolved Oxygen, DO μM), and the Weights Used in the Optimum Multiparameter Analysis[a]

Properties	CDW	LSSW	HSSW	OMP Weight
θ (°C)	1.00	−1.88	−1.88	1.073
S	34.75	34.30	34.56	1.073
DO (μM)	192	330	326	2.250
Mass conservation	1	1	1	2.250

[a]CDW = Circumpolar Deep Water; LSSW = Low-Salinity Shelf Water; and HSSW = High-Salinity Shelf Water.

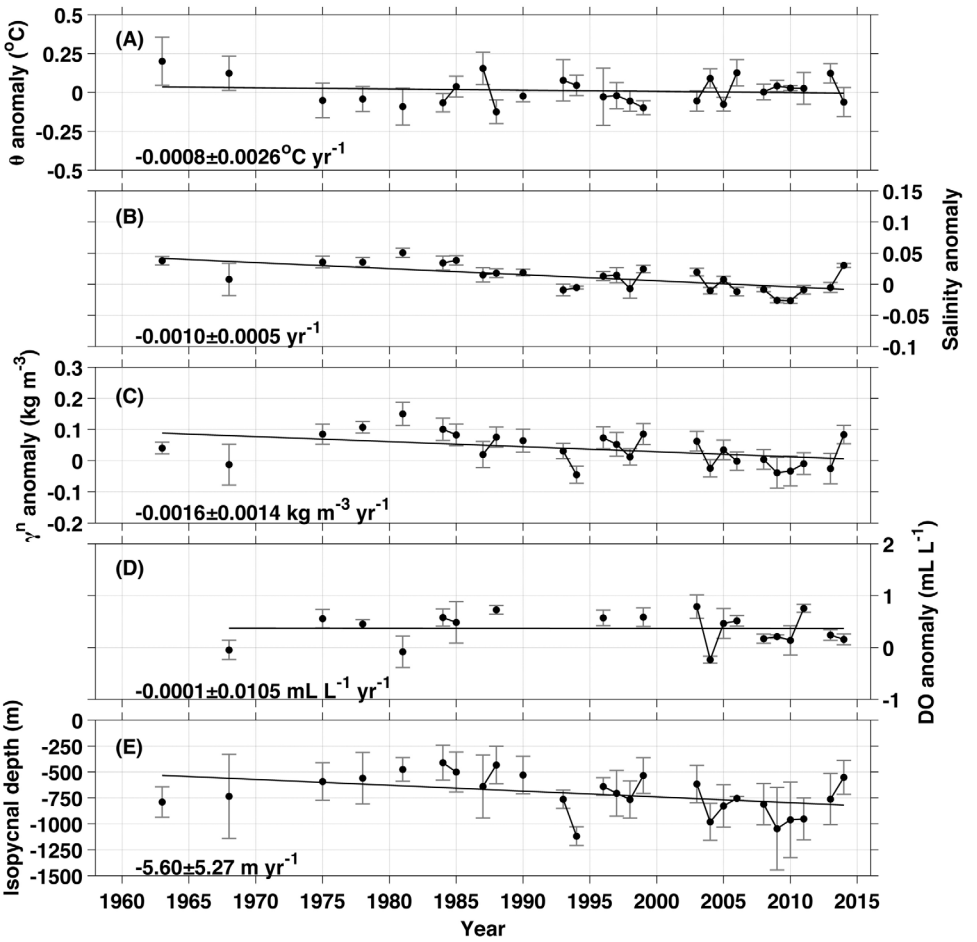

Figure 4. Anomaly time series of the hydrographic parameters for the deep waters ($\gamma^n > 28.27$ kg m^{-3} and depth > 800 m) in the central basin of the Bransfield Strait. (a) Potential temperature, (b) salinity, (c) neutral density, (d) dissolved oxygen, and (e) the depth of the 28.27 kg m^{-3} isopycnal. The trends are listed by linear fits (black lines) within each plot. If the confidence bound is lower than the trend, the result is statistically significant at the 95% level ($p \leq 0.05$).

1990s and 2000s, θ did not change in the central basin. Below 1000 m, the θ differences between decades were smaller and generally were not significant (less than ~0.01°C; Figure 2a). In the eastern basin, the θ differences below 1000 m were higher than in the central basin (Figure 3a), and the profile from the 2010s was ~0.1°C warmer than that from the 2000s and ~0.2°C warmer than that from the 1980s. The 1990s profile of the eastern basin did not reach the deep depths of the basin.

The decadal *S* profiles of the central and eastern basins (Figures 2b and 3b, respectively) showed substantial differences with depth. Generally, the highest *S* values (i.e., saltiest deep waters) of the study period were observed in the 1980s, whereas the lowest *S* values were observed in the 2000s in both basins (Figures 2b and 3b). The salinity differences were greater in the eastern basin (e.g., approximately 0.025 between the 2000s and 2010s; Figure 3b).

The 1980s γ^n profile (Figures 2c and 3c) featured higher values in both basins compared with the rest of the analyzed decades (except in the eastern basin in the 1990s). Lower γ^n values were found in the 2000s and 2010s. The differences between the densest and the lightest decades were ~0.1 kg m^{-3} in both basins, and these changes decreased along with depth (Figures 2c and 3c). The isopycnal of 28.27 kg m^{-3} deepened over time from ~550 m during the 1980s to ~800 m after the 2000s in the central basin (Figure 2c) and from ~800 m in the 1980s and 1990s to ~1300 m in the 2010s in the eastern basin (Figure 3c).

3.2. Temporal Variability in the Bransfield Strait Deep Water Masses (1960s–2010s)

For this analysis, we considered the full period from the 1960s to 2010s ($\gamma^n \geq 28.27$ kg m^{-3} and depth > 800 m as described in section 2.3) to identify trends in the hydrographic properties from the

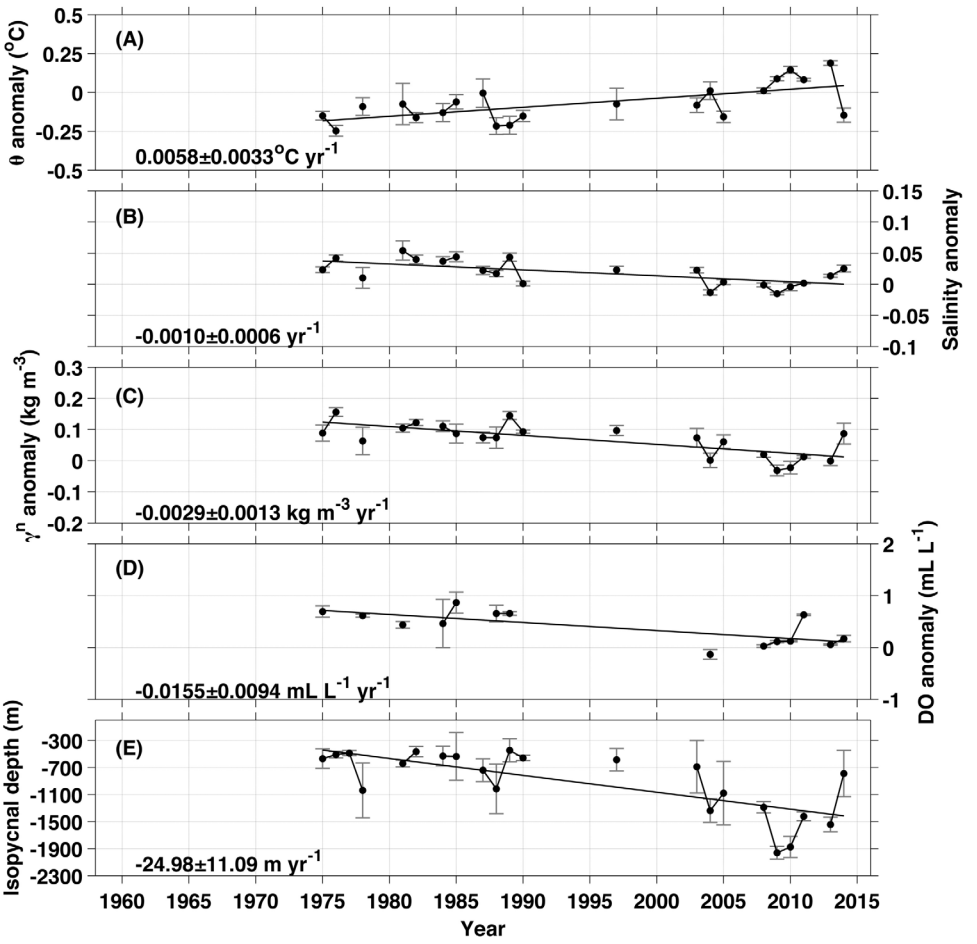

Figure 5. Same as in Figure 4 but for the eastern basin of the Bransfield Strait. Note that the scales between the central basin and the eastern basin are different.

anomaly time series in the central and eastern basins. In the central basin, between 1963 and 2014, decreased values of θ, S, and γ^n were recorded for the deep layers at rates of -0.0008 ± 0.0026°C yr^{-1}, -0.0010 ± 0.0005 yr^{-1}, and -0.0016 ± 0.0014 kg m^{-3} yr^{-1}, respectively (Figures 4a–4c; all of the trends and their statistical significance are summarized in Table 2). In the eastern basin between 1975 and 2014, increased θ values were observed at rate of $+0.0058 \pm 0.0033$°C yr^{-1} and decreased S and γ^n values were observed at rates of -0.0010 ± 0.0006 yr^{-1} and -0.0029 ± 0.0013 kg m^{-3} yr^{-1}, respectively (Figures 5a–5c and Table 2). The DO content decreased in both basins, although it was statistically significant only in the eastern basin (-0.0155 ± 0.0094 mL L^{-1} yr^{-1}). However, less DO data were available compared with the θ

Table 2. Hydrographic Trends and Confidence Bounds (at 95% Level) Observed in the Central Basin (1963–2014) and Eastern Basin (1975–2014) of the Bransfield Strait, as well as the Normalized and Detrended Potential Temperature, Salinity, and Neutral Density Correlations with the SAM Index (August–October of the Previous Year)[a]

Trends	Central Basin	Eastern Basin
θ (°C yr^{-1})	-0.0008 ± 0.0026 (0.54)	$+0.0058 \pm 0.0033$ (0.00)
S (yr^{-1})	-0.0010 ± 0.0005 (0.00)	-0.0010 ± 0.0006 (0.00)
γ^n (kg m^{-3} yr^{-1})	-0.0016 ± 0.0014 (0.03)	-0.0029 ± 0.0013 (0.00)
DO (mL L^{-1} yr^{-1})	-0.0001 ± 0.0105 (0.98)	-0.0155 ± 0.0094 (0.00)
Isopycnal depth (m yr^{-1})	-5.60 ± 5.27 (0.04)	-24.98 ± 11.09 (0.00)
Hydrographic properties (1980–2014)	Correlation with the SAM index (average from August–October of the previous year)	
θ	+0.41 (0.06)	+0.50 (0.03)
S	−0.56 (0.01)	−0.58 (0.00)
γ^n	−0.62 (0.00)	−0.68 (0.00)

[a]*p*-Values are shown in parentheses.

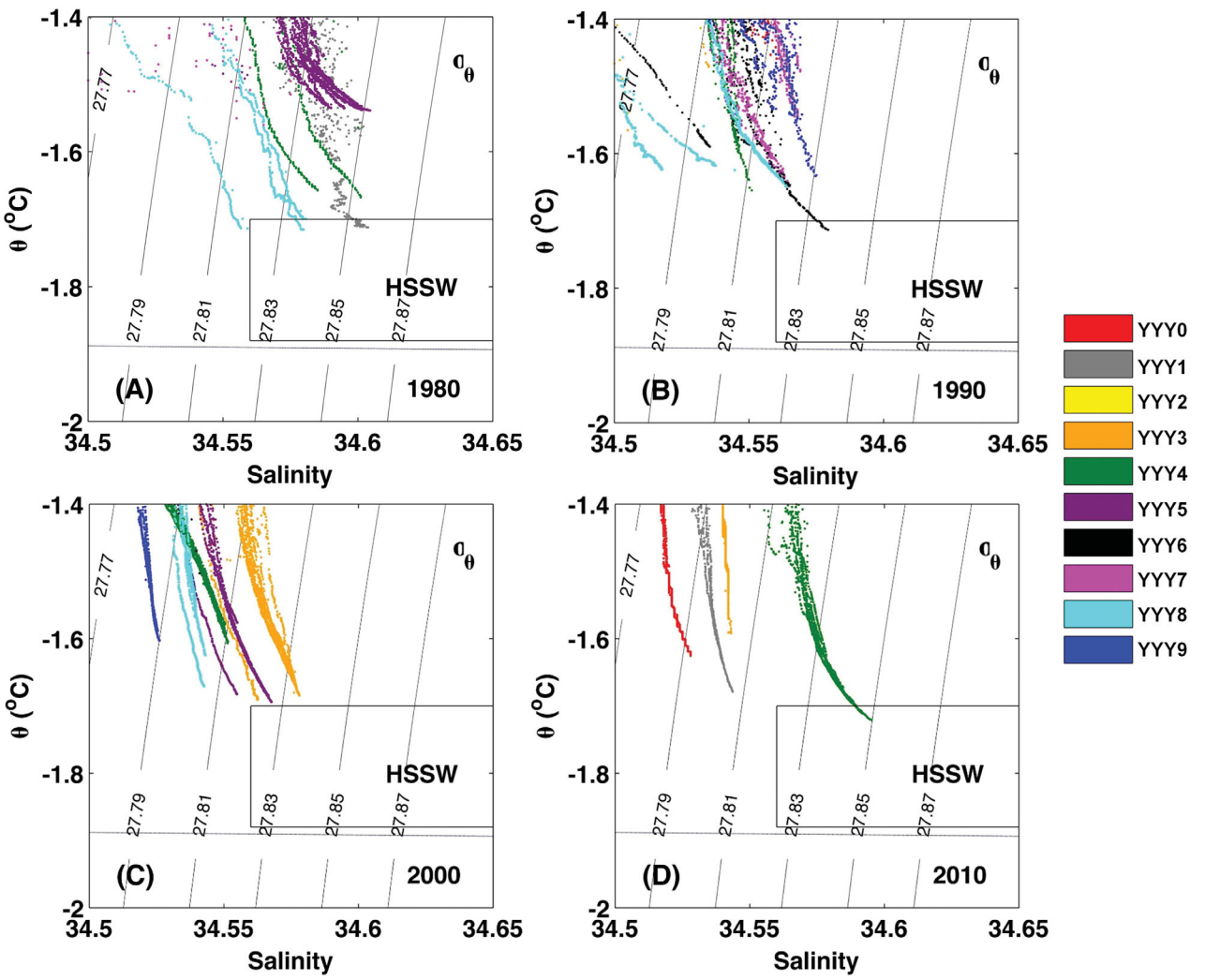

Figure 6. θ-S diagrams for the coldest deep water masses ($\theta \leq -1.4$°C) in the central basin of the Bransfield Strait. The numbers in the colored legend represent the year in the (a) 1980s, (b) 1990s, (c) 2000s, and (d) 2010s. The isopycnal lines represent potential density. The rectangles represent the thermohaline characteristics of the High-Salinity Shelf Water (HSSW) from the Weddell Sea. The quasi-horizontal lines represent the freezing point of seawater.

and S data in the 1990s, which may have influenced the trend analysis (Figure 5d). The calculated S values presented an almost monotonic increase in both basins from 2009–2010 to the end of records (Figures 4b and 5b). Finally, the 28.27 kg m^{-3} isopycnal depth deepened over the study period in both the central and the eastern basins at rates of -5.60 ± 5.27 m yr^{-1} and -24.98 ± 11.09 m yr^{-1}, respectively (Figures 4e and 5e).

The central basin is more easily ventilated and can trap more dense waters relative to the eastern basin (Figures 6 and 7), which is associated with the well-preserved shelf water from the Weddell Sea that sinks in that region. The central basin showed high thermohaline variability among years within each decade from the 1980s to the 2010s (Figure 6). Within the 1980s, 1990s, and 2000s (in particular), these dense and cold waters generally tended to become less saline and less dense between the beginning and the end of each decade (Figures 6b and 6c). Conversely, the coldest deep waters tended to become more saline and dense within the first half of the 2010s (Figure 6d). In 2014, the θ and S parameters of the deep, cold waters reached the thermohaline property values of the HSSW from the Weddell Sea (Figure 6d), which has not been observed since 1996 in this region (Figure 6b). However, these patterns were not as clear in the eastern basin (Figure 7), which may have been caused by the connections between the eastern basin and the Powell Basin and the Northeast Channel, which favor the exchange and mixing with the surrounding waters [e.g., *Gordon et al.*, 2000], thus attenuating the properties of the shelf waters that eventually enter the basin.

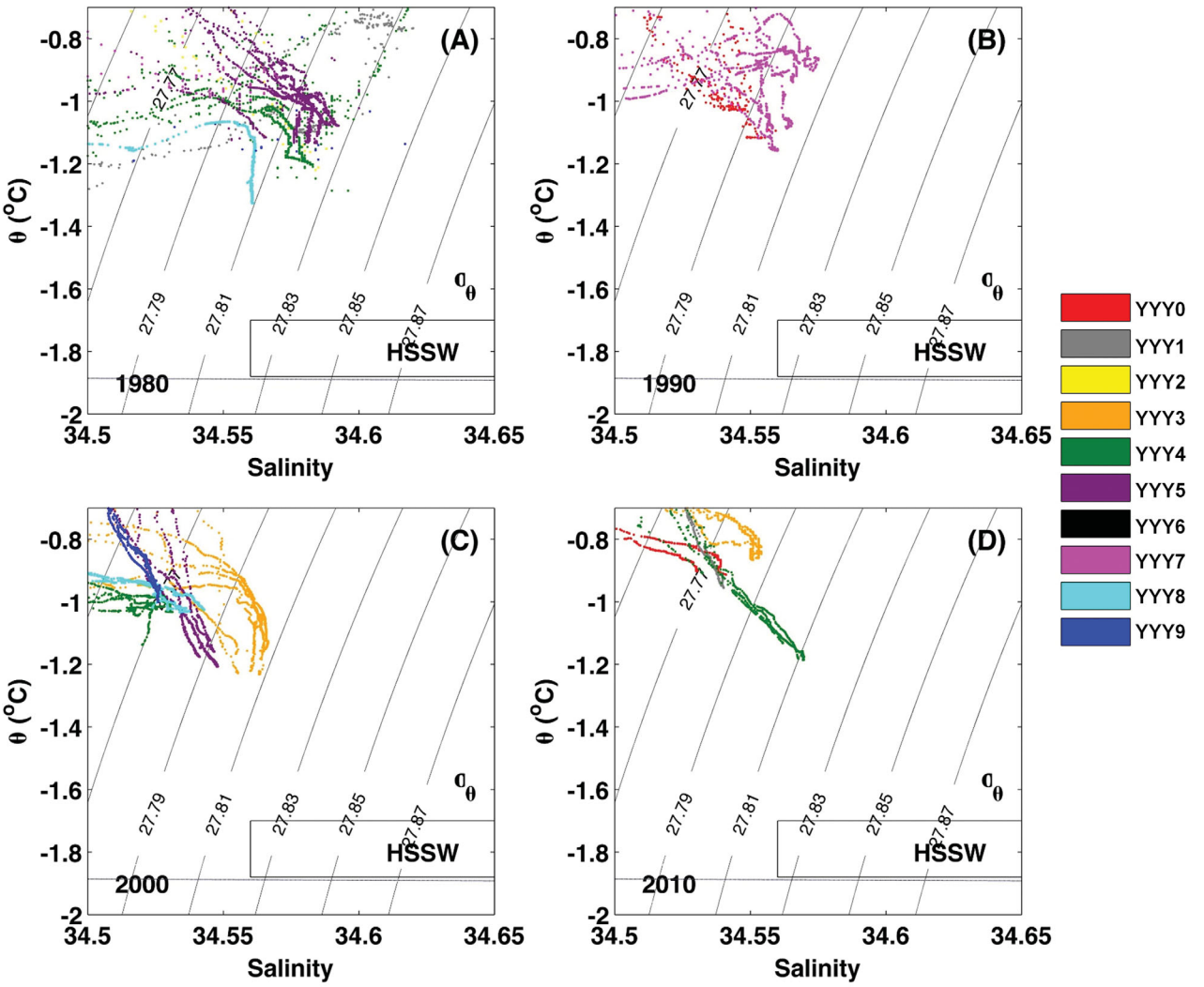

Figure 7. Same as in Figure 6 but for the eastern basin of the Bransfield Strait. Note that the scales between the central basin and the eastern basin are different.

However, despite all of the differences among the basins, the deep waters of the eastern basin also presented a cold and saline water mass in 2014 (Figure 7d) similar to that observed in the central basin (Figure 6d).

3.3. Mixing of the Bransfield Strait Deep Water Masses

We quantified the contributions of the water mass sources to the deep water in the central and eastern basins (depths > 800 m) using the high-resolution CTD data set from the GOAL repeated hydrographic section. The OMP analysis revealed a reduction of ∼10% and ∼30% in the CDW and LSSW contributions, respectively, to the total water composition between 2004 and 2014 in the central basin (Figure 8). In the eastern basin, the proportions of CDW and LSSW decreased by ∼5–10% and ∼20–25%, respectively, during the same period. Between 2009 and 2010, the LSSW represented ∼40% of the total mixture in the central basin and contributed to the basin's lower salinity values during these 2 years (Figure 4b). The proportion of HSSW increased by ∼20–30% in both basins during the study period (Figure 8). According to the OMP results, the interannual variability in the deep waters of Bransfield Strait was strongly affected by changes in the proportions of source water masses.

3.4. Correlations Between the SAM and the Bransfield Strait Deep Water Masses Variability

We tested the correlations between the variability of the normalized and detrended thermohaline properties of the Bransfield Strait and the SAM index (using it as a proxy for the regional winds patterns). The

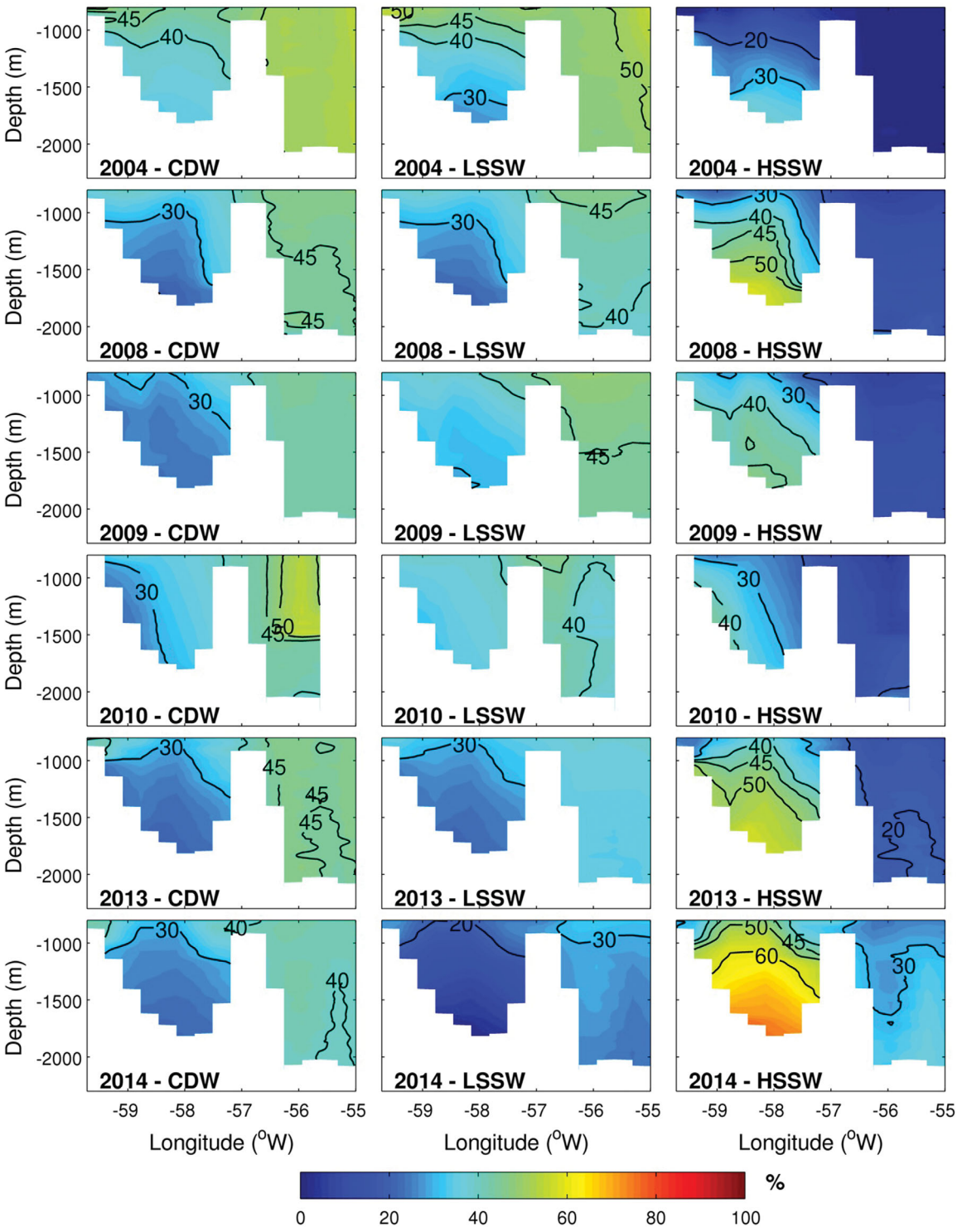

Figure 8. Mixture proportions of distinct water masses below 800 m in the central and eastern basins of the Bransfield Strait. (left) The Circumpolar Deep Water (CDW), (middle) the Low Salinity Shelf Water (LSSW), and (right) the High-Salinity Shelf Water (HSSW). (top to bottom) The years between 2004 and 2014, for which we performed the OMP analysis.

highest correlation presented a time lag of ~5 months, considering that most of the data were collected from December to March, and this lag is consistent with the effect of wind stress on the thermohaline characteristics of the AABW exported from the Weddell Sea [e.g., *Jullion et al.*, 2010]. The normalized and detrended S and γ^n time series of the central basin were negatively correlated with the August–September–

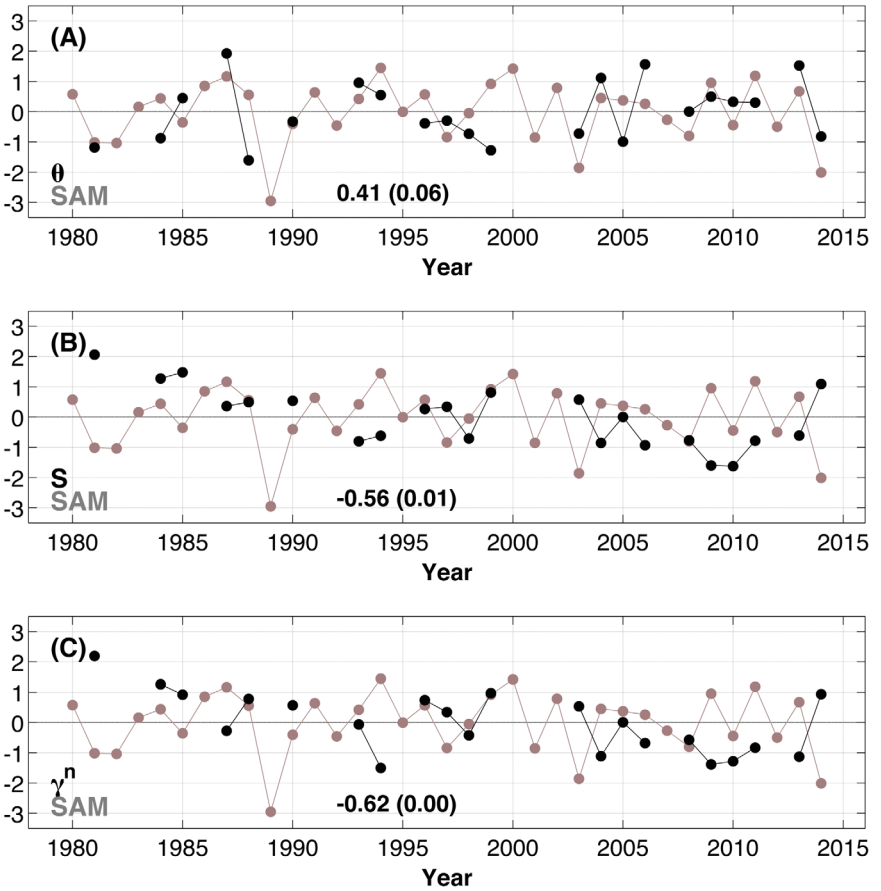

Figure 9. Temporal evolution of the normalized and detrended SAM index and the following oceanic properties: (a) θ, (b) S, and (c) γ^n for the central basin. The SAM index (gray) is the average of August–October of each year. The hydrographical properties are in black. The correlation coefficients and P-value (in parenthesis) between the SAM index and θ, S, and γ^n are indicated within each plot. The correlations are calculated between the hydrographic properties and the previous year of the SAM. Note that the SAM index is advanced by one year in the figure.

October-averaged SAM index of the previous year ($r = -0.56$ and -0.62, respectively; both at the 99% statistical significance level), whereas θ was positively correlated ($r = +0.41$; $p = 0.06$) (Figures 9a–9c; for the eastern basin, please, see Table 2). Therefore, the positive phase of the SAM at the end of austral winter and the beginning of austral spring is correlated with a decrease in the salinity and density of the central basin deep waters of the Bransfield Strait the following summer, whereas the opposite occurs during the SAM negative phase, which is correlated with increases in the salinity and density of the central basin deep waters of the Bransfield Strait.

4. Discussion

4.1. Long-Term Trends of the Deep Water of the Bransfield Strait

Previous studies compared only specific cruises (with limited hydrographical stations available) or evaluated the Bransfield Strait as a whole without differentiating between basins [e.g., *Wilson et al.*, 1999; *Garcia and Mata*, 2005; *Azaneu et al.*, 2013]. In the present study, we expanded the number of available data from different cruises, grouped the cruise data into their respective summers and extended the analysis until the GOAL cruise of February 2014. The inclusion of the novel high-resolution data from GOAL led to a much more robust analysis. The long-term time series included in the present work revealed statistically significant negative trends for S and γ^n in the deep waters of both the central and the eastern basins of the Bransfield Strait (Table 2). The thermohaline characteristics of the water masses of the strait are more uniform below 800 m [e.g., *Gordon et al.*, 2000], and the criteria used here to select only these deep water masses helped to attenuate the effects of sampling bias between years. If a constant trend is assumed

throughout the entire analyzed period, the total amount of change in θ, S, and γ^n is higher than the instrumental accuracy (see section 2). Our salinity trends are also greater than the threshold of ± 0.0005 yr^{-1}, which is considered a significant change for the majority of the oceans [*Boyer et al*., 2005] and ensures that the freshening trends observed in the present work are robust for evaluating hydrographic changes in the deep Bransfield Strait. During the whole period analyzed, the time series showed a high degree of interannual variability of the hydrographic properties, including between 2003 and 2014 in which the GOAL stations were predominant (Figure 1b).

These findings are generally consistent with those of previous studies in the region and provide an update of the thermohaline long-term trends in the deep waters of the Bransfield Strait, as well as new insights into the causes of changes in the deep oceans. *Wilson et al*. [1999] found a net heat flux of -4.90 W m^{-2} and a freshwater input of $+1.08$ m m^{-2} in an analysis of five sparse surveys of the central and eastern basins between 1963 and 1995, and their results indicated a decrease of θ and S until 1995. In turn, *Garcia and Mata* [2005] documented a freshening of -0.0014 yr^{-1} and warming of $+0.0027$°C yr^{-1} for the central basin between 1980 and 2005. Here, only the eastern basin showed a warming trend in the period from 1975–2014 of $+0.0058 \pm 0.0033$°C yr^{-1} (Table 2). By restricting our time series of the central basin from 1980 to 2005, a decrease in θ is still observed (-0.0017°C yr^{-1}), and if the same criteria of *Garcia and Mata* [2005] are used, an increase in θ of $+0.0002$°C yr^{-1} is observed, although this value is not statistically significant. Moreover, the S and γ^n values of the central basin decreased at rates of -0.0014 yr^{-1} ($p = 0.02$) and -0.0028 kg m^{-3} yr^{-1} ($p = 0.12$), respectively, between the 1980 and 2005 and at rates of -0.0014 yr^{-1} ($p = 0.01$) and -0.0033 kg m^{-3} yr^{-1} ($p = 0.11$), respectively, when the criteria of *Garcia and Mata* [2005] are used. The difference between the results of *Garcia and Mata* [2005] and those of the present work is related mainly to the differences between the methods and the extended time series used in our study. Conversely, *Azaneu et al*. [2013] found a decrease in θ, S, and γ^n values at rates of -0.0278°C yr^{-1}, -0.0012 yr^{-1}, and -0.0013 kg m^{-3} yr^{-1}, respectively, from 1958 to 2010 for all of the Bransfield Strait. Hence, high thermohaline interannual variability was observed in the Bransfield Strait (Figures 4 and 5), and all of the relevant studies concluded that the deep waters are experiencing a long-term freshening and lightening regardless of the different timescales or approaches used.

The freshening trends of the dense waters observed here within the central and eastern basin (Table 2) were consistent with the trends observed by *Azaneu et al*. [2013] in the shelf waters of the southeastern Weddell Sea (-0.0013 yr^{-1}, 1958–2010) and by *Schmidtko et al*. [2014] in the shelf waters of the western Weddell Sea (-0.0010 g kg^{-1} yr^{-1}; presented in absolute salinity; 1980s–2010s). Our results are lower than the estimates of *Hellmer et al*. [2011] of -0.0053 yr^{-1} for the entire water column between 1989 and 2006 in the northwestern Weddell Sea shelf. However, *Hellmer et al*. [2011] used only data from three cruises (three repeated hydrographical stations) in the Weddell Sea continental shelf region, which may account for their considerably higher variability.

Several regional ocean and cryosphere processes have been proposed to explain the freshening trends observed in shelf waters around Antarctica [e.g., *Jacobs and Giulivi*, 2010; *Hellmer et al*., 2011; *Azaneu et al*., 2013; *Schmidtko et al*., 2014]. The Antarctic Peninsula has experienced intense ice shelf mass loss events over the last 50 years [e.g., *Cook and Vaughan*, 2010; *Shepherd et al*., 2012]. For example, the western continental shelf of the Weddell Sea received a freshwater input of -37.2 Gt yr^{-1} between 2003 and 2008 from the basal melting of the Larsen Ice Shelves system at the eastern Antarctic Peninsula [*Rignot et al*., 2013]. Therefore, it is expected that the Weddell Sea shelf water carries a cold, fresh signal from the ice shelf melting from the eastern Antarctic Peninsula into the Bransfield Strait deep layers [e.g., *Kusahara and Hasumi*, 2014] because of circulation around the tip of the Antarctic Peninsula [*Gordon et al*., 2000; *von Gyldenfeldt et al*., 2002; *Thompson et al*., 2009; *Palmer et al*., 2012]. Using a simple volume budget of freshwater for the central basin (considering depths $>$ 800 m; for a full description of the method) [see *Jullion et al*., 2013], an input of $\sim$17 Gt freshwater ($\sim$0.33 Gt yr^{-1}) would be necessary to account for the freshening trend observed in the region for the period from 1963 to 2014. Thus, from a long-term perspective, the thermohaline variations of the incoming source water masses play a pivotal role in driving changes in the thermohaline characteristics of the Bransfield Strait deep waters. In this context, the Bransfield Strait can reflect and preserve the signal of shelf water freshening occurring in the western Weddell Sea shelf region, thus highlighting the importance of continuous observations of its deep basin in relation to the long-term monitoring of the Southern Ocean [e.g., *Meredith et al*., 2015].

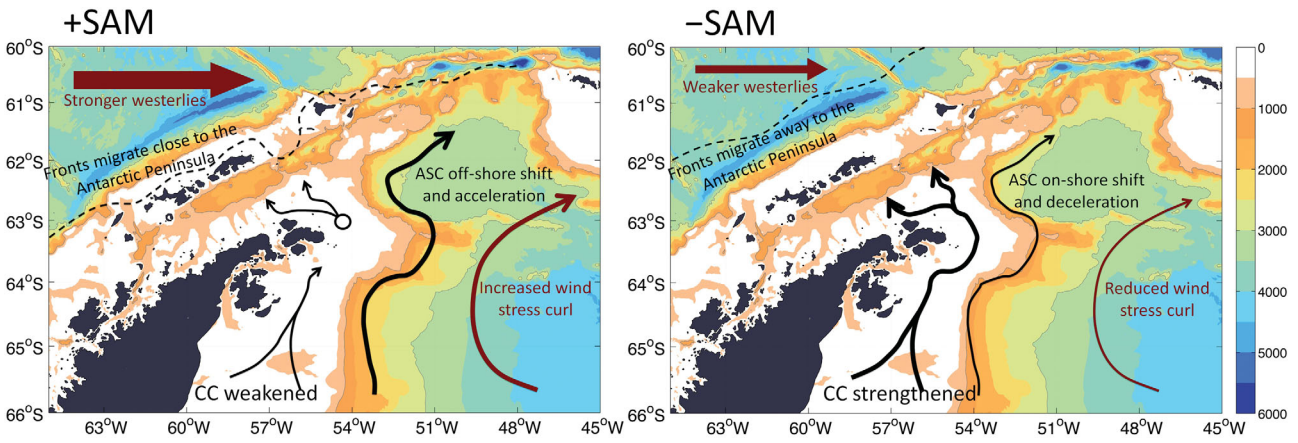

Figure 10. Schematic summary of the effects of the SAM on the tip of the Antarctic Peninsula region. During positive SAM phases (left), the westerlies are stronger and push the fronts close to the Antarctic Peninsula, the wind stress curl over the Weddell Sea, and the Antarctic Slope Current (ASC) are stronger and accelerated, the coastal currents (CC) are weakened, and a local variety of shelf water sinks into the Bransfield Strait. In a negative SAM phase (right), the opposite occurs, with the westerlies weakening, the fronts moving away from the Antarctic Peninsula, the wind stress curl reducing, the ASC decelerating, and the CC strengthening; these conditions allow for the transport of a denser variety of shelf water into the Bransfield Strait.

Additionally, significant changes were not observed in the DO of the central basin (Figure 4d and Table 2), suggesting that the ventilation rate of the Bransfield Strait has not changed from 1963 to 2014. At the eastern basin, a significant decrease in the DO content of the deep waters was observed between 1975 and 2014; however, these results may not be reliable because of the lack of data between the 1990s and most of the 2000s. A significant deepening of the 28.27 kg m^{-3} isopycnal was observed in both basins, and it corresponded to depth changes of the isopycnal of -5.60 ± 5.27 m yr^{-1} for the central basin (Figure 4e) and -24.98 ± 11.09 m yr^{-1} for the eastern basin (Figure 5e). To our knowledge, evidence related to deep water shrinkage in this region has not been reported prior to this study. The observed shrinking of the Bransfield Strait deep waters is related to the freshening and lightening trends because freshening can drive water mass contraction even if the overall formation rate remains unchanged [e.g., *van Wijk and Rintoul*, 2014]. Thus, the Bransfield Strait is another region that reflects the observed contraction of the deep, dense water masses around the Antarctic continent over the last 50 years [e.g., *Azaneu et al.*, 2013; *van Wijk and Rintoul*, 2014].

4.2. Interannual Variability of the Deep Waters of the Bransfield Strait

The Bransfield Strait deep waters exhibited a high degree of thermohaline interannual variability (Figures 4–8). This pattern was observed even during the GOAL period (2003–2014), when the oceanographic properties were closely sampled with high temporal resolution (Figures 4, 5 and 8). During this period, an increase of ~0.06 in S was observed between 2010 and 2014 in the central basin. To evaluate the interannual variability during this period, an OMP analysis was performed for a repeated hydrographic transect along the central and eastern basins (Figure 1b). The salinification process of the deep waters between 2010 and 2014 was caused by an increase in the contribution of HSSW and a corresponding decrease in LSSW of approximately 20% in the deep water mixture (Figure 8). These changes in the mixture were consistent with a decrease in the discharge and runoff of freshwater from the tributary glaciers around the former Larsen A Ice Shelf [*Rott et al.*, 2014]. The lower quantity of freshwater injected into the system decreased the dilution of the shelf waters in the region and contributed to the prevalence of more saline deep waters after 2010 in the central basin of the Bransfield Strait. Therefore, changes in the proportion of the source water masses from the Weddell Sea shelves appear to play a role in the high degree of interannual variability of the Bransfield Strait water masses over short-term periods. Although we have not provided an analysis of the process, changes in CDW intrusions [e.g., *Moffat et al.*, 2009; *Dinniman et al.*, 2012] within the Bransfield Strait may also contribute to changes in the deep water mixture ratio in the region.

The local atmospheric effects related to SAM may also influence the interannual variability of the water properties in the Bransfield Strait because of variations among the water masses entering the region. The negative correlations between the normalized and detrended S (-0.56 and -0.58 for the central and eastern basins, respectively) and γ^n (-0.62 and -0.68 for the central and eastern basins, respectively) in both

basins (Table 2) indicate that when the SAM is in its positive phase at the end of austral winter and the beginning of austral spring (~5 months lag), the salinity and density of the deep waters of the central basin of the Bransfield Strait decrease the following summer, whereas the opposite is true when the SAM is in its negative phase. During positive SAM phases, both the Weddell Gyre and the Antarctic Slope Current are accelerated by the strengthening of the negative cyclonic wind stress curl upon the region [*Youngs et al*., 2015] (Figure 10), thus limiting the connection between the Weddell Sea and the areas west of the Antarctic Peninsula because of a shift of the southern boundary of the Antarctic Circumpolar Current front [*Renner et al*., 2012]. Moreover, a strengthening of the Weddell Gyre under positive SAM phases shifts the isopycnals at the slope and facilitates the export of cold, saline shelf waters into the deep Weddell Sea [*Mckee et al*., 2011] via cross-slope flow at a zero time lag [*Kerr et al*., 2012]. In the periods when the cyclonic wind stress curl is strengthened, the coastal current at the western Weddell Sea appears to weaken [e.g., *Youngs et al*., 2015]; in addition, ocean models have also shown a weakening of the coastal currents during persistent southward shifting westerly winds, which is an effect of positive SAM phases, diminishing its propagation northward by the warming of the shelf waters [e.g., *Spence et al*., 2014]. A weakened coastal current may transport a variety of shelf water to the Bransfield Strait that is less dense and may originate in the northwestern Weddell Sea (Figure 10). However, during SAM negative phases (which are associated with less intense wind stress curls), the Weddell Gyre and Antarctic Slope Current are weakened, and the coastal currents may be intensified, which may transport saline and dense waters from a southern origin that were not exported to the deep Weddell Sea (Figure 10) [*Mckee et al*., 2011].

5. Summary and Conclusions

In this study, we investigated the thermohaline variability within the Bransfield Strait using a hydrographic data set spanning the period from the 1960s–2010s. Our results showed that the deep water masses ($\gamma^n \geq 28.27$ kg m^{-3} and depth > 800 m) of the central (1963–2014) and eastern (1975–2014) basins experienced statistically significant (95% confidence level) freshening -0.0010 ± 0.0005 yr^{-1} and -0.0010 ± 0.0006 yr^{-1}, respectively and lightening (-0.0016 ± 0.0014 kg m^{-3} yr^{-1} and -0.0029 ± 0.0013 kg m^{-3} yr^{-1}, respectively), which supports the findings of previous investigations in the area [e.g., *Wilson et al*., 1999; *Garcia and Mata*, 2005; *Azaneu et al*., 2013]. Thus, thermohaline variations in the source water masses are likely the main causes of the long-term trends observed in the hydrographic properties of the deep waters of Bransfield Strait. In addition, we reported that the deep layers in the Bransfield Strait shrank at rates of -5.60 ± 5.27 m yr^{-1} for the central basin (1963–2014) and -24.98 ± 11.09 m yr^{-1} for the eastern basin (1975–2014).

Changes in the proportions of the source water masses have been attributed to the high degree thermohaline interannual variability found within the deep waters of the Bransfield Strait. For instance, between 2010 and 2014, an increase of ~20% in the HSSW and a corresponding decrease in the LSSW were responsible for the observed increase in salinity of ~0.06 in the central basin (Figure 8). However, how changes in the proportion of shelf (HSSW and LSSW) and modified CDW affect the formation of regional varieties of AABW in the shelf-break of the northwestern Weddell Sea have not been determined, although they are likely related to the reduced contribution (~20%) of Weddell Sea Bottom Water into the deep Weddell Sea in previous periods [*Kerr et al*., 2009].

Both the S and γ^n fields are negatively correlated with the SAM index. The local effects associated with a positive SAM phase likely promote decreases in S values in the Bransfield Strait deep waters. Conversely, regional coastal currents are expected to intensify during negative SAM phases, which transport more saline and denser shelf waters into the Bransfield Strait as observed for the years after 2010 (Figure 9b). Because the majority of the dense waters in Bransfield Strait originate in the western Weddell Sea continental shelves [*Gordon et al*., 2000; *von Gyldenfeldt et al*., 2002] and the regional bathymetric features can trap and limit the mixing of those dense waters with surrounding waters, the Bransfield Strait is considered an important area for studying the thermohaline changes of the Weddell Sea shelf water, which is an important precursor of AABW [e.g., *van Caspel et al*., 2015]. If the freshening and lightening trends identified here continue, the γ^n of the central basin deep water masses may decrease to values less than 28.27 kg m^{-3} (upper limit of the AABW) in ~65 years, which means that a less dense variety of AABW will likely be formed in the western Weddell Sea.

Therefore, increased sampling and modeling activities of the Southern Ocean are essential for a better understanding of its long-term hydrographic variability. Long-term ocean reanalysis products or regional modeling simulations can be helpful in this regard; however, a primary assessment of their current representation must be performed to identify possible discrepancies [e.g., *Azaneu et al*., 2014; *Dotto et al*., 2014]. Finally, the effects of the recent changes in shelf water salinity on the volume of AABW exported to the global ocean remain an open question for future investigations. Thus, considering the imminent risk of collapse of the Larsen C Ice Shelf [e.g., *Holland et al*., 2015], continued sampling of the Bransfield Strait deep waters must be performed to monitor future changes of the Weddell Sea shelf waters.

Acknowledgments

This study provides a contribution to the activities of the Brazilian High Latitudes Oceanography Group (GOAL; www.goal.furg.br), which is part of the Brazilian Antarctic Program (PROANTAR). GOAL has been funded by and/or has received logistical support from the Brazilian Ministry of the Environment (MMA), the Brazilian Ministry of Science, Technology and Innovation (MCTI), and the Council for Research and Scientific Development of Brazil (CNPq) through grants from the International Polar Year SOS-CLIMATE project (550370/2002-1; 520189/2006-0), the Brazilian National Institute of Science and Technology of Cryosphere (INCT-CRIOSFERA; 573720/2008-8) and POLARCANION, NAUTILUS, and CAPES/CMAR2 projects (556848/2009-8; 405869/2013-4, 23038.001421/2014-30). T. S. Dotto acknowledges financial support from CAPES Foundation and from CNPq (grant 232792/2014-3). R. Kerr, M. M. Mata, and C. A. E. Garcia acknowledge, respectively, CNPq researcher grants 302604/2015-4, 306896/2015-0, and 311943/2015-2. We thank Gareth Marshall for the SAM index data (http://www.nerc-bas.ac.uk/icd/gjma/sam.html) and the Alfred-Wegener Institute, NOAA World Ocean Database and all of the scientists who participated in the data collection and provided it freely available through the websites www.pangaea.de and www.nodc.noaa.gov. The GOAL data set will be added to the Brazilian National Oceanographic Data Archive Center (BNDO; http://www.mar.mil.br/dhn/chm/oceanografia/bndo.html) and is provided by request. We also thank the Brazilian Navy, especially the crew, officials, and scientist onboard of the Brazilian Navy vessels N.Ap.Oc. *Ary Rongel* (2003–2012) and N.Po. *Almirante Maximiano* (2013–2014), for providing logistical support during all GOAL cruises.

References

Azaneu, M., R. Kerr, M. M. Mata, and C. A. E. Garcia (2013), Trends in the deep Southern Ocean (1958–2010): Implications for Antarctic Bottom Water properties and volume export, *J. Geophys. Res. Oceans*, *118*, 4213–4227, doi:10.1002/jgrc.20303.

Azaneu, M., R. Kerr, and M. M. Mata (2014), Assessment of the representation of Antarctic bottom water properties in the ECCO2 reanalysis, *Ocean Sci.*, *10*, 923–946, doi:10.5194/os-10-923-2014.

Boyer, T. P., S. Levitus, and J. I. Antonov (2005), Linear trends in salinity for the World Ocean, 1955–1998, *Geophys. Res. Lett.*, *32*, L01604, doi:10.1029/2004GL021791.

Boyer, T. P., et al. (2013), *World Ocean Database 2013, NOAA Atlas NESDIS 72*, edited by S. Levitus and A. Mishonov, 209 pp., Silver Spring, Md., doi:10.7289/V5NZ85MT.

Carmack, E. C. (1974), A quantitative characterization of water masses in the Weddell Sea during summer, *Deep Sea Res. Oceanogr. Abstr.*, *74*, 431–443, doi:10.1016/0011-7471(74)90092-8.

Carmack, E. C., and T. D. Foster (1975), On the flow of water out of the Weddell Sea, *Deep Sea Res. Oceanogr. Abstr.*, *22*, 711–724, doi:10.1016/0011-7471(75)90077-7.

Clowes, A. J. (1934), Hydrology of the Bransfield Strait, Discovery Rep., 9, pp. 1–64.

Collares, L. L., M. M. Mata, J. Arigony, and R. Kerr (2015), Icebergs identification and tracking using ASAR images in the Northwestern Weddell Sea, Antarctica, *Rev. Soc. Bras. Cartogr. Geod. Fotogram. Sens. Remoto*, *67*, 569–589.

Cook, A. J., and D. G. Vaughan (2010), Overview of areal changes of the ice shelves on the Antarctic Peninsula over the past 50 years, *Cryosphere*, *4*(1), 77–98, doi:10.5194/tc-4-77-2010.

Cook, A. J., A. J. Fox, D. G. Vaughan, and J. G. Ferrigno (2005), Retreating Glacier fronts on the Antarctic Peninsula over the past Half-Century, *Science*, *308*, 541–544, doi:10.1126/science.1104235.

Dinniman, M. S., J. M. Klinck, and E. E. Hofmann (2012) Sensitivity of circumpolar deep water transport and ice shelf basal melt along the west Antarctic Peninsula to changes in the winds, *J. Clim.*, *25*, 4799–4816, doi:10.1175/JCLI-D-11-00307.1.

Dotto, T. S., R. Kerr, M. M. Mata, M. Azaneu, I. Wainer, E. Fahrbach, and G. Rohardt (2014), Assessment of the structure and variability of Weddell Sea water masses in distinct ocean reanalysis products, *Ocean Sci.*, *10*, 523–546, doi:10.5194/os-10-523-2014.

Durack, P. J., S. E. Wijffels, and R. J. Matear (2012), Ocean salinities reveal strong global water cycle intensification during 1950 to 2000, *Science*, *335*, 455–458, doi:10.1126/science.1212222.

Garcia, C. A. E., and M. M. Mata (2005), Deep and bottom water variability in the central basin of Bransfield Strait (Antarctica) over the 1980–2005 period, *CLIVAR Exchanges*, *10*(4), 48–50.

Gordon, A. L., and W. D. Nowlin Jr. (1978), The basin waters of the Bransfield Strait, *J. Phys. Oceanogr.*, *8*, 258–264, doi:10.1175/1520-0485(1978)008 < 0258:TBWOTB>2.0.CO;2.

Gordon, A. L., M. Mensch, D. Zhaoqian, W. M. Smethie, and J. de Bettencourt (2000), Deep and bottom water of the Bransfield Strait eastern and central basins, *J. Geophys. Res.*, *105*(C5), 11,337–11,346, doi:10.1029/2000JC900030.

Hellmer, H. H., O. Huhn, D. Gomis, and R. Timmermann (2011), On the freshening of the northwestern Weddell Sea continental shelf, *Ocean Sci.*, *7*, 305–316, doi:10.5194/os-7-305-2011.

Heywood, K. J., et al. (2014), Ocean processes at the Antarctic continental slope, *Philos. Trans. R. Soc. A*, *372*, 20130047, doi:10.1098/rsta.2013.0047.

Hofmann, E. E, J. M. Klinck, C. M. Lascara, and D. A. Smith (1996), Water mass distribution and circulation west of the Antarctic Peninsula and including Bransfield Basin, Foundations for Ecological Research West of the Antarctic Peninsula, *Antarct. Res. Seri.*, *70*, 61–800.

Holland, P. R., A. Brisbourne, H. F. J. Corr, D. McGrath, K. Purdon, J. Paden, H. A. Fricker, F. S. Paolo, and A. H. Fleming (2015), Oceanic and atmospheric forcing of Larsen C Ice-Shelf thinning, *Cryosphere*, *9*, 1005–1024, doi:10.5194/tc-9-1005-2015.

Huhn, O., H. H. Hellmer, M. Rhein, C. Rodehacke, W. Roether, M. Schodlok, and M. Schröder (2008), Evidence of deep- and bottom-water formation in the western Weddell Sea, *Deep Sea Res., Part II*, *55*(8), 1098–1116, doi:10.1016/j.dsr2.2007.12.015.

Jacobs, S. S., and C. F. Giulivi (2010), Large multidecadal salinity trends near the Pacific–Antarctic continental margin, *J. Clim.*, *23*, 4508–4524, doi:10.1175/2010JCLI3284.1.

Johnson, D. R., T. P. Boyer, H. E. Garcia, R. A. Locarnini, O. K. Baranova, and M. M. Zweng (2013) *World Ocean Database 2013 User's Manual*, edited by S. Levitus and A. Mishonov, *NODC Int. Rep. 22*, NOAA Print. Off., Silver Spring, Md., 172 pp. [Available at http://www.nodc.noaa.gov/OC5/WOD13/docwod13.html.]

Jullion, L., S. C. Jones, A. C. Naveira Garabato, and M. P. Meredith (2010), Wind-controlled export of Antarctic bottom water from the Weddell Sea, *Geophys. Res. Lett.*, *37*, L09609, doi:10.1029/2010GL042822.

Jullion, L., A. Naveira Garabato, M. Meredith, P. Holland, P. Courtois, and B. King (2013), Decadal freshening of the Antarctic bottom water exported from the Weddell Sea, *J. Clim.*, *26*, 8111–8125, doi:10.1175/JCLI-D-12-00765.1.

Kerr, R., M. M. Mata, and C. A. E. Garcia (2009), On the temporal variability of the Weddell Sea Deep water masses, *Antarct. Sci.*, *21*(4), 383–400, doi:10.1017/S0954102009001990.

Kerr, R., K. J. Heywood, M. M. Mata, M. M., and C. A. E. Garcia (2012), On the outflow of dense water from the Weddell and Ross Seas in OCCAM model, *Ocean Sci.*, *8*, 369–388, doi:10.5194/os-8-369-2012.

Kusahara, K., and H. Hasumi (2014), Pathways of basal meltwater from Antarctic ice shelves: A model study, *J. Geophys. Res. Oceans*, *119*, 5690–5704, doi:10.1002/2014JC009915.

Leffanue, H., and M. Tomczak (2004), Using OMP analysis to observe temporal variability in water mass distribution, *J. Mar. Res.*, *48*, 3–14, doi:10.1016/j.jmarsys.2003.07.004.

Marshall, G. (2003), Trends in the Southern annular mode from observations and reanalyses, *J. Clim.*, *16*, 4134–4143, doi:10.1175/1520-0442(2003)016 < 4134:TITSAM>2.0.CO;2.
Marshall, G. J., P. A. Stott, J. Turner, W. M. Connolley, J. C. King, and T. A. Lachlan-Cope (2004), Causes of exceptional atmospheric circulation changes in the Southern Hemisphere, *Geophys. Res. Lett.*, *31*, L14205, doi:10.1029/2004GL019952.
McKee, D. C., X. Yuan, A. L. Gordon, B. A. Huber, and Z. Dong (2011), Climate impact on interannual variability of Weddell Sea Bottom Water, *J. Geophys. Res.*, *116*, C05020, doi:10.1029/2010JC006484.
Meredith, M. P., et al. (2015), Southern Ocean, [in "State of Climate in 2014"], *Bull. Am. Meteorol. Soc.*, *96*(7), S157–S160.
Moffat, C., B. Owens, and R. C. Beardsley (2009), On the characteristics of circumpolar deep water intrusions to the west Antarctic Peninsula continental shelf, *J. Geophys. Res.*, *114*, C05017, doi:10.1029/2008JC004955.
Nicholls, K. W., S. Østerhus, K. Makinson, T. Gammelsrod, and E. Fahrbach (2009), Ice-ocean processes over the continental shelf of the southern Weddell Sea, Antarctica: A review, *Rev. Geophys.*, *47*, RG3003, doi:10.1029/2007RG000250.
Niiler, P. P., A. Amos, and J.-H. Hu (1991), Water masses and 200 m relative geostrophic circulation in the western Bransfield Strait region, *Deep Sea Res., Part A*, *38*, 943–959, doi:10.1016/0198-0149(91)90091-S.
Orsi, A. H., T. Whitworth III, and W. D. Nowlin (1995), On the meridional extent and fronts of the Antarctic Circumpolar Current, *Deep Sea Res., Part I*, *42*(5), 641–673, doi:10.1016/0967-0637(95)00021-W.
Orsi, A. H., G. C. Johnson, and J. L. Bullister (1999), Circulation, mixing and production of Antarctic bottom water, *Prog. Oceanogr.*, *43*, 55–109, doi:10.1016/S0079-6611(99)00004-X.
Palmer, M., D. Gomis, M. M. Flexas, G. Jordà, L. Jullion, T. Tsubouchi, A. C. Naveira Garabato (2012), Water mass pathways and transports over the South Scotia Ridge west of 50°W, *Deep Sea Res., Part I*, *59*, 8–24, doi:10.1016/j.dsr.2011.10.005.
Purkey, S. G., and G. C. Johnson (2013), Antarctic bottom water warming and freshening: Contributions to sea level rise, ocean freshwater budgets, and global heat gain, *J. Clim.*, *26*, 6105–6122, doi:10.1175/JCLI-D-12-00834.1.
Renner, A. H. H., S. E. Thorpe, K. J. Heywood, E. J. Murphy, J. L. Watkins, and M. P. Meredith (2012), Advective pathways near the tip of the Antarctic Peninsula: Trends, variability and ecosystem implications, *Deep Sea Res., Part I*, *63*, 91–101, doi:10.1016/j.dsr.2012.01.009.
Rignot E., S. Jacobs, J. Mouginot, and B. Scheuchl (2013), Ice-shelf melting around Antarctica, *Science*, *341*, 266–270, doi:10.1126/science.1235798.
Robertson, R., M. Visbeck, A. L. Gordon, and E. Fahrbach (2002), Long-term temperature trends in the deep waters of the Weddell Sea, *Deep Sea Res., Part II*, *49*(21), 4791–4806, doi:10.1016/S0967-0645(02)00159-5.
Rott, H., D. Floricioiu, J. Wuite, S. Scheiblauer, T. Nagler, and M. Kern (2014), Mass changes of outlet glaciers along the Nordensjköld Coast, northern Antarctic Peninsula, based on TanDEM-X satellite measurements, *Geophys. Res. Lett.*, *41*, 8123–8129, doi:10.1002/2014GL061613.
Sangrà, P., C. Gordoa, M. Hernández-Arencibia, A. Marrero-Díaz, A. Rodríguez-Santana, A. Stegner, A. Martínez-Marrero, J. L. Pelegrí, and T. Pichon (2011), The Bransfield current system, *Deep Sea Res., Part I*, *58*, 390–402, doi:10.1016/j.dsr.2011.01.011.
Schmidtko, S., K. J. Heywood, A. F. Thompson, and S. Aoki (2014), Multidecadal warming of Antarctic waters, *Science*, *346*, 1227–1231, doi:10.1126/science.1256117.
Shepherd, A., et al. (2012), A reconciled estimate of ice-sheet mass balance, *Science*, *338*, 1183–1189, doi:10.1126/science.1228102.
Spence, P., S. M. Griffies, M. H. England, A. McC. Hogg, O. A. Saenko, and N. C. Jourdain (2014), Rapid subsurface warming and circulation changes of Antarctic coastal waters by poleward shifting winds, *Geophys. Res. Lett.*, *41*, 4601–4610, doi:10.1002/2014GL06061.
Thompson, A. F., K. J. Heywood, S. E. Thorpe, A. H. H. Renner, and A. Trasviña (2009), Surface circulation at the tip of the Antarctic Peninsula from drifters, *J. Phys. Oceanogr.*, *39*, 3–26, doi:10.1175/2008JPO3995.1.
Tomczak, M., and D. G. B. Large (1989), Optimum multiparameter analysis of mixing in the thermocline of the eastern Indian Ocean, *J. Geophys. Res.*, *94*(C11), 16,141–16,149, doi:10.1029/JC094iC11p16141.
Tomczak, M., and S. Liefrink (2005), Interannual variations of water mass volumes in the Southern Ocean, *J. Atmos. Ocean Sci.*, *10*(1), 31–42, doi:10.1080/17417530500062838.
van Caspel, M., M. Schröder, O. Huhn, H. H. Hellmer (2015), Precursors of Antarctic bottom water formed on the continental shelf off Larsen ice shelf, *Deep Sea Res., Part I*, *99*, 1–9, doi:10.1016/j.dsr.2015.01.004.
van Wijk, E. M., and S. R. Rintoul (2014), Freshening drives contraction of Antarctic bottom water in the Australian Antarctic basin, *Geophys. Res. Lett.*, *41*, 1657–1664, doi:10.1002/2013GL058921.
von Gyldenfeldt, A.-B., E. Fahrbach, M. A. García, M. Schröder (2002), Flow variability at the tip of the Antarctic Peninsula, *Deep Sea Res., Part II*, *49*(21), 4743–4766, doi:10.1016/S0967-0645(02)00157-1.
Weppernig, R., P. Schlosser, S. Khatiwala, and R. G. Fairbanks (1996), Isotope data from Ice Station Weddell: Implications for deep water formation in the Weddell Sea, *J. Geophys. Res.*, *101*(C11), 25,723–25,739, doi:10.1029/96JC01895.
Whitworth, T., W. Nowlin, A. Orsi, R. A. Locarnini, and S. G. Smith (1994), Weddell Sea shelf water in the Bransfield Strait and Weddell Scotia confluence, *Deep Sea Res., Part I*, *41*(4), 629–641, doi:10.1016/0967-0637(94)90046-9.
Wilson, C., G. P. Klinkhammer, and C. S. Chin (1999), Hydrography within the central and east basins of the Bransfield Strait, Antarctica, *J. Phys. Oceanogr.*, *29*, 465–479.
Youngs, M. K., A. F. Thompson, M. M. Flexas, and K. J. Heywood (2015) Weddell sea export pathways from surface drifters, *J. Phys. Oceanogr.*, *45*, 1068–1085, doi:10.1175/JPO-D-14-0103.1.
Zhou, M., P. P. Niiler, and J.-H. Hu (2002), Surface currents in the Bransfield and Gerlache Straits, Antarctica, *Deep Sea Res., Part I*, *49*(2), 267–280, doi:10.1016/S0967-0637(01)00062-0.